



## Research Article

# Impact of Dust and Degradation on the Electrical Properties of PV Panels

Samir Tabet<sup>a,b</sup>, Razika Ihaddadene<sup>a,c\*</sup>, Belhi Guerira<sup>d</sup>, Nabila Ihaddadene<sup>a,c</sup>

<sup>a</sup> Department of Mechanical Engineering, Faculty of Technology, University of Med Boudiaf, M'sila, Algeria.

<sup>b</sup> Laboratory of Materials and Mechanics of Structure L.M.MS, University of Med Boudiaf, M'sila, Algeria.

<sup>c</sup> Laboratory of Renewable Energy and Sustainable Development L.R.E.S.E, University of Mentouri Brothers, Constantine, Algeria.

<sup>d</sup> Laboratory of Mechanical Engineering L.M.G, University Mohamed Khider, Biskra, Algeria.

### PAPER INFO

#### Paper history:

Received: 05 November 2022

Revised: 01 November 2022

Accepted: 11 December 2022

#### Keywords:

Dust Accumulation,  
Solar PV Performance,  
Degradation Rate,  
Degradation Mechanisms,  
Electrical Characteristics

### ABSTRACT

Dust accumulation on PV surface panels is a crucial factor affecting their performance. It is more frequently noted in the desert zones. The effect of dust on the electrical behavior of damaged PV panels was investigated in this study. Three panels are used: the degraded panels (with and without dust) and the reference panels; they are located in an industrial zone with a continental climate (Bordj Bou Arréridj, Algeria). The I-V and P-V characterization and degradation mechanism visualization are used. Also, a numerical simulation was conducted to calculate the five parameters of the three modeled PV panels (diode ideality factor (a), series resistance (Rs), Shunt resistance (Rp), photocurrent (I<sub>pv</sub>), and diode saturation current (I<sub>0</sub>)). These parameters were utilized for the first time to study the impact of dust on their degradation rate and the PV panel behavior. The degradation rate and the annual degradation rate of each parameter are affected by dust differently. The power degradation rate is increased by 5.45%. The I<sub>sc</sub> and I<sub>max</sub> degradation rates are climbed by 6.97% and 6.0%, respectively. V<sub>max</sub> and V<sub>oc</sub> degradation rates decrease by 1.20% and 0.35%, respectively. Dust increased the rate of degradation for a, I<sub>ph</sub>, and I<sub>0</sub> by 4.12%, 6.99%, and 68.17%, respectively. For Rs and Rp, the degradation rate was reduced by 4.51% and 20.01%, respectively. An appropriate netting approach must be considered because dust, even in non-desert areas and industrial zones, has a significant impact on the electrical characteristics degradation of a PV panel.

<https://doi.org/10.30501/jree.2023.367573.1491>

## 1. INTRODUCTION

Solar chimneys, photovoltaic (PV), and concentrated-solar power plants are a few examples of solar utilizations that have been observed in the electricity industry (Franzese et al., 2020). Thermoelectric (TE) technology is an approach that directly converts the heat available from automobiles, industries, etc. into electricity without any intermediate conversion (Seebeck effect and Peltier effect) (Subbarama et al., 2019). Similarly, TEG converts electricity into thermal energy for the required heating or cooling applications. In order to achieve the high conversion efficiency and spread its wings for all applications, extensive research into the TE technology and its materials was conducted (Subbarama et al., 2019). A recent invention involving the combination of TEG with solar concentrator technologies to generate electricity has been welcomed (Sahu et al., 2021).

Electricity can be produced directly from chemical energy in reactants by electrochemical devices known as fuel cells. Proton Exchange Membrane Fuel Cells (PEMFC) have received significant attention among all fuel cell types and have been viewed as the best option for both portable electronics like laptops and future transportation applications. Numerous

studies have looked into different PEMFC performance facets in relation to operating parameters. The results of numerical simulations indicated that the presence of a substantial Gas Diffusion Layer (GDL) could enhance the movement of species across porous layers, increasing the performance of fuel cells (Ahmadi et al., 2015). Besides, the circular and elliptical channel cross-sections produced higher current densities, as compared to the traditional model (Ashkan et al., 2014).

The PV application has been developed in terms of its technology and electricity production, leading to price reduction (Darwish et al., 2013). The susceptibility of this technology to various outside climate parameters like humidity levels, temperature, wind, clouds, and lack of solar radiation in some regions is a drawback (Chaichan & Kazem, 2016). These climatic parameters have a significant impact on the efficiency of PV systems (Ihaddadene et al., 2022; Sendhil & Subbarama, 2019).

The impact of dust on PV performance on a global scale was recognized in (Mani & Phillai, 2010; Chaichan et al., 2015; Kazem et al., 2017; Vidyanandan, 2017; Chen et al., 2020). By serving as a barrier between the PV and the radiation, dust attenuates the transmittance of cellular glazing (Chaichan et al., 2015) in dusty countries and in desert regions. In dusty

\*Corresponding Author's Email: [razika.ihaddadene@univ-msila.dz](mailto:razika.ihaddadene@univ-msila.dz) (R. Ihaddadene)

URL: [https://www.jree.ir/article\\_165693.html](https://www.jree.ir/article_165693.html)



countries and desert regions, it reduces cellular glazing transmittance ([Chaichan et al., 2015](#)) by acting as a barrier between the PV and the radiation. Dust collects particles with a diameter less than 500 m ([Tanesab et al., 2019](#); [Pan et al., 2019](#)). Its composition, structural morphology, and deposition are related to its localization characteristics ([Aissa et al., 2017](#)). Noting that many contaminants and dirt, such as sand, dust, pollutants, smoke, dirt, pollen, and so on that result from human activities are suspended in the air and these have been expressed as dust in most studies. PV module performance is heavily influenced by the particle size and surface density of dust deposited on the panels ([Styszko et al., 2019](#)). Indeed, studies on this phenomenon have been reported for different solar energy technologies, in particular PV, CSP, CPV, and thermal solar ([Menoufi, 2017](#); [Chaichan et al., 2018](#)).

Dust collection on a panel may cause the cells to warm up, acting as a barrier to the power produced ([Kazem et al., 2017](#)). This tendency results in a major decline in efficiency and even the formation of a hot spot, which may eventually harm the PV module ([Tripathi et al., 2017](#)). However, there have been numerous suggestions for cleaning PV to increase efficiency. The cleaning of PV modules cannot rely on occasional rain and should be planned based on the regular density accumulated. PV system tilt-angle and orientation, ambient temperature and humidity, site characteristics, dust properties, wind speed velocity, and glazing characteristics are all factors that influence dust settlement ([Mani & Phillai, 2010](#)). Specifically, in arid areas where the use of water is challenging due to its scarcity, the presence of relatively high humidity in the air combined with dust may result in the development of thin surface layers on the PV. These layers cannot be removed by wind or any conventional cleaning techniques ([Hachicha et al., 2019](#)). The wind decelerates after a dust storm, and granules start to gather and settle. Consequently, due to their size and weight, small molecules can stay in the atmosphere for days or even months ([Namdari et al., 2018](#)).

The performance of PV systems is impacted by soiling and condensation in arid regions with high dust frequencies and high relative humidity levels, which can significantly reduce their power production. Recently, Amer et al. ([Amer et al., 2022](#)) developed a new technique to lessen the impact of moisture and soiling accumulation on PV performance using superhydrophobic and superhydrophilic coating on the PV module surface. The effect of condensation and the buildup of soiling, which could damage the performance of the PV panels and lower their efficiencies, was successfully reduced by this technique.

Due to its assistance, especially in primarily desert nations which make up the solar belt zone and its environs, the effects of dust deposits on PV panel surfaces have been extensively researched. Based on the plant location, it was found that the daily reduction in PV productivity in hot climates without precipitation may reach 0.2%/day or reduce PV productivity by 56.2% per year ([Kimber et al., 2007](#)). The findings revealed a 31–35% decline in PV performance in August 2010 in Jordan ([Essalameh et al., 2013](#)). The impact of dust on PV cell efficiency was examined in Baghdad (Iraq) ([Mani & Phillai, 2010](#)). The reported finding shows that dirt and pollution reduced the performance of PV despite a brief time without washing. The efficiency of the filthy and contaminated PV cells was about 12 % less than that of the clean cell. Prolonged exposure times cause the aggregation of dust particles ([Waved](#)

[et al., 2017](#)). Five distinct types of dust (carbon, cement, and various classes of limestone) were used in an indoor experiment to examine if they could impact the output power of solar cells ([El-Shoboksky & Hussein, 1993](#)). They discovered that the PV efficiency was considerably worsened by finer particles.

Another study examined the effects of traffic-related pollutants and the dirt arising from them. This study discovered that this type of dust and pollutants accumulates quickly, clearly reducing the performance of PV by 20% ([Dorobantu et al., 2017](#)). The study findings also indicate that even a very thin layer of this kind of dirt buildup can result in a 40% decrease in PV efficiency. Significantly less short-circuit current is produced, especially at high dust density ([Hachicha et al., 2019](#)). Following a 1.7%/g/m<sup>2</sup> decline, a linear relation is found between normalizing PV power and dust collection on the PV surface. Both indoor and outdoor circumstances were validated for this correlation.

It should be mentioned that studies on the impact of dust on solar panels are frequently carried out in desert areas. Also, degraded panels were not used in these studies. According to the findings of the current research, maximum power ( $P_{max}$ ), short-circuit current ( $I_{sc}$ ), open-circuit voltage ( $V_{oc}$ ), and shape factor (FF) all degrade at different rates. Several studies on the effect of dust on the degradation of resistances ( $R_s$  and  $R_p$ ) are also mentioned. The present paper investigates the impact of dust on the degraded panels under outdoor conditions in an industrial zone located in a non-desert region characterized by a continental climate.

The first part of this work is devoted to the effect of dust and degradation on all the parameters of the curves (I-V and P-V), including  $I_{sc}$ ,  $V_{oc}$ ,  $P_{max}$ ,  $I_{max}$ , and  $V_{max}$ . Of note, the evolution of these curves is performed using a PV simulator, which allows them to be plotted precisely under normal conditions (1000 W/m<sup>2</sup> and 25 °C). Furthermore, degradation mechanisms of the degraded panel in this zone are visualized.

The second section of this paper employs a numerical simulation to compute five electrical parameters ( $a$ ,  $R_s$ ,  $R_p$ ,  $I_{pv}$ , and  $I_0$ ) of the three panels namely degraded (with and without dust) and reference panels. This simulation uses a mathematical model to simulate the behavior of the PV panel. For the first time, degraded panels are used in this simulation. The obtained results allow calculating the degradation rate and annual degradation rate of these five parameters as well as evaluating the effect of dust on their degradation. Of note, the two mentioned rates have been calculated for the first time ever.

## 2. MATERIALS AND METHODS

This study concentrates on the monocrystalline PV modules (CEM235P-60) installed on the roof of Condor company in Bordj Bou Arréridj (BBA-Algeria), as shown in Figure 1 in detail. Despite being mounted on the roof, these panels did not produce any electricity. They are made up of 60 cells that are linked in series and have the properties of their manufacturers under typical conditions, as shown in Table 1. One panel, known as a "degraded panel with dust," has been degrading naturally for six years (it has not been cleaned). It is referred to as a "degraded panel without dust" after cleaning. Of note, in the experiments, soiling from rain and airborne dust particles, particularly in this industrial zone, constitutes the majority of the dirt accumulation. A new panel with the same settings was utilized as a reference panel.

BBA is located on a high plateau in the north-east of Algeria (Figure 2). It is placed between 35° and 37° parallels of latitude north and between the meridians of longitudes 4° and 5° east. It is characterized by a continental climate that offers hot temperatures in the summer and very cold temperatures in winter, among the lowest in Algeria. The annual rainfall ranges from 300 to 700 mm. Winters are long, extremely cold, and frequently cloudy in BBA, whereas summers are brief, hot, dry, and mostly clear. The average annual temperature ranges from 1°C to 34°C, rarely falling below -3°C or rising above 37°C ([Weather Spark, 2022](#)).



**Figure 1.** Used panels from left to right : (a) Reference panel, (b) degraded panel with dust and (c) degraded panel without dust.

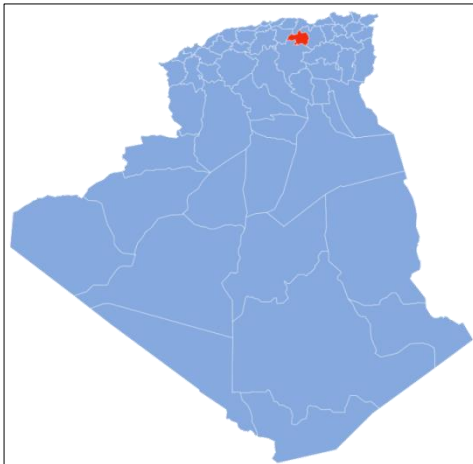


**Figure 2.** Geographical location of BBA region in Algeria ([Wikipedia, 2022](#)).

The performance of photovoltaic panels was evaluated using a photovoltaic simulator at Condor Company in BBA (Algeria) (Figure 3). This LED sun simulator (simulator of the A+A+A++ class), known as Ecosun Plus, was designed to carry out semi-automatic quality checks based on artificial lighting and a replication of the normal operating state for the module (STC). The high LED output allows for the recreation of solar irradiance in comparable settings, simulating the solar spectrum in accordance with IEC 60904 editions 2 and 3.

The solar simulator measures the courbes I-V and P-V, one of many variables that are crucial for determining the module power and efficiency. With the option to repeat tests without losing time between them, the same simulator offers an

immediate response, good stability, and repeatability. In other words, the solar simulator is crucial for determining potential power losses in finished modules and checking the quality of the modules in the course of solar panel testing. Ecosun Plus can be exploited for all existing solar cell technologies, including HIT, PERC, MWT, bifaciales, and hybrid silicon cells and also photovoltaic modules of all shapes and sizes, from crystal to "couche mince" for back-contact cells. In this study, this simulator was used for investigating solar panels to give the I-V and P-V curves under the STC test.



**Figure 3.** LED Sun Simulator in Condor company.

The degradation rate and the annual degradation rate of the degraded panel with dust are denoted by  $R_{DD}$  and  $R_{AD}$ , respectively. The degradation rate and the annual degradation rate of the degraded panel without dust (cleaned) are given as  $R_{DC}$  and  $R_{ADC}$ , respectively. The degradation rate and the annual degradation rate of each performance parameter (open circuit voltage ( $V_{oc}$ ), short-circuit current ( $I_{sc}$ ), maximum power ( $P_{max}$ ), maximum voltage ( $V_{max}$ ), and maximum current ( $I_{max}$ )) in a standard condition are calculated using the following equations ([Bandou et al., 2015](#), [Bouaichi et al., 2019](#)):

$$R_{DD(C)}(Y) = \left(1 - \frac{Y}{Y_0}\right) \times 100 \quad (1)$$

$$R_{ADD(C)}(Y) = \frac{R_{DD(C)}(Y)}{N} \quad (2)$$

The performance parameters of the degraded panel with dust or without dust (cleaned) and reference panel are denoted by  $Y = [I_{sc}, V_{oc}, P_{max}, V_{max}, I_{max}]$  and  $Y_0 = [P_{max0}, V_{max0}, I_{max0}, I_{sc0}, V_{oc0}]$ , respectively.  $N$  is the year number of module exposure duration in real conditions. The reference performance parameters and the degraded performance parameters (with and without dust) are determined experimentally using the Led Sun simulator in standard conditions.

**Table 1.** The electrical parameters of the used PV panel at STC ([Condor, 2022](#)).

Parameters	Values.
Nominal power ( $P_{max}$ )	235 W
Short-circuit current ( $I_{sc}$ )	8.4 A
Open-circuit voltage ( $V_{oc}$ )	37.4 V
Maximum power current ( $I_{max}$ )	7.78 V
Maximum power tension ( $V_{max}$ )	30.2 V
Cells number ( $N_s$ )	60
Temperature coefficient of $I_{sc}$ ( $k_I$ )	+0.06%/°C
Temperature coefficient of $V_{oc}$ ( $k_V$ )	+0.32%/°C
Temperature coefficient of $P_{max}$ ( $k_P$ )	+0.41%/°C

### 3. RESULTS AND DISCUSSION

#### 3.1. Degradation rates

After analyzing the degraded PV panel (with and without dust) and reference PV panel in the STC using the Ecosun Plus simulator, the I-V and P-V curves of each panel are plotted, the parameter values ( $I_{sc}$ ,  $V_{oc}$ ,  $P_{max}$ ,  $I_{max}$ , and  $V_{max}$ ) extracted for each case, and the degradation rate and the annual degradation rate calculated for the degraded panels (with and without dust).

##### A. Degraded panel without dust

The I-V and P-V evolutions of the degraded panel (without dust) and the reference panel are illustrated in Figures 4 and 5, respectively. All the electrical parameters ( $I_{sc}$ ,  $V_{oc}$ ,  $P_{max}$ ,  $I_{max}$ , and  $V_{max}$ ) are degrading at different rates, as noted in Table 2.

The power rate degradation was 4.32% with an annual degradation rate of 0.86%/y. These findings are consistent with the Algerian power degradation rate in several climates, including the Saharan environment (Adrar), where annual power degradation rate ranges from 0.85%/y to 2.26%/y (Bandou et al., 2015), and the Mediterranean climate in the Bouzareah, where annual power degradation rate varies from 0.82%/y to 1.47%/y (Belhaouas, 2022). In Adrar region, higher power degradation rates are observed (3.33%/year to 4.64%/year) (Kahoul et al., 2017) than that noted in BBA with continental climate conditions.  $V_{oc}$  has the lowest degradation rate (0.91%) with an annual degradation rate of 0.18%/y. Both currents  $I_{sc}$  (1.17%-0.23%/y) and  $I_{max}$  (1.13%-0.23%/y) experienced similar degradation rates. A high degradation rate for  $V_{max}$  (3.24%-0.65%/y) is noted.

##### B. Degraded panel with dust

Figures 6 and 7 illustrate the I-V and P-V evolutions of the reference and degraded panels with dust, respectively. The two curves I-namely V and P-V of the degraded panel with dust have the same pattern as those of the reference panel. In this case, the power rate degradation was 9.50 % with an annual degradation rate of 1.90%/y. As a result, the presence of dust reduced the maximum power generated by the degraded panel by 5.45 %.

The degradation rate of  $V_{oc}$  for the panel degraded with dust was 0.56%, with an annual degradation rate of 0.11%/y and a minimal rise of 0.35 % compared to the degraded panel without dust.

The highest degradation rates were registered for the currents, namely  $I_{sc}$  (8.06%-1.61%/y) and  $I_{max}$  (7.65%-1.53%/y), with the increase rates of 6.97% and 6.0% in the presence of dust. The degradation rate of  $V_{max}$  for the degraded panel with dust was 2.08% (0.42%/y) with a reduction of 1.20% in the presence of dust.

As noted, the presence of dust affects the degradation rate and the annual degradation rate of all the parameters ( $I_{sc}$ ,  $V_{oc}$ ,  $P_{max}$ ,  $I_{max}$ ,  $V_{max}$ ) with different values, and this finding in agreement with the results of Hachicha et al. (2019). Also, in this case, the  $I_{sc}$  degradation rate was more significant than  $V_{oc}$  degradation rate; this finding is consistent with high dust density (Hachicha et al., 2019) and various industrial dusts (Dorobantu et al., 2017). Therefore, dust accumulation had no significant impact on  $V_{oc}$  as seen in Figures 6 and 7. (Andrea, 2019) found similar results using different industrial dusts (fertilizer, gypsum,

aggregate crusher, and coal mine industries) under a tropical climatic condition of Arusha, Tanzania.

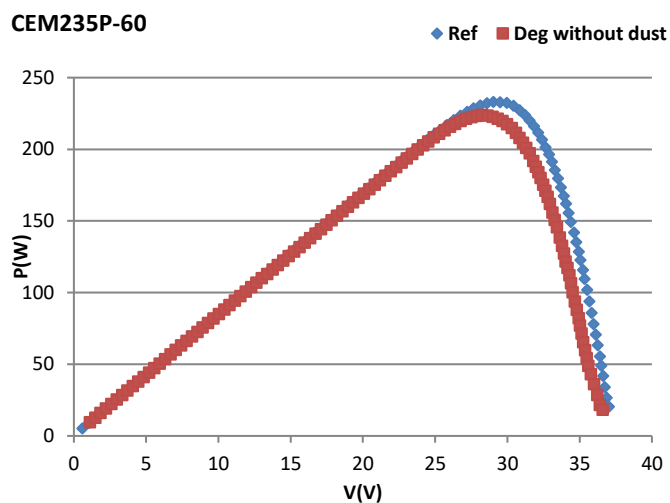


Figure 5. P-V curves for the reference panel and degraded without dust panel.

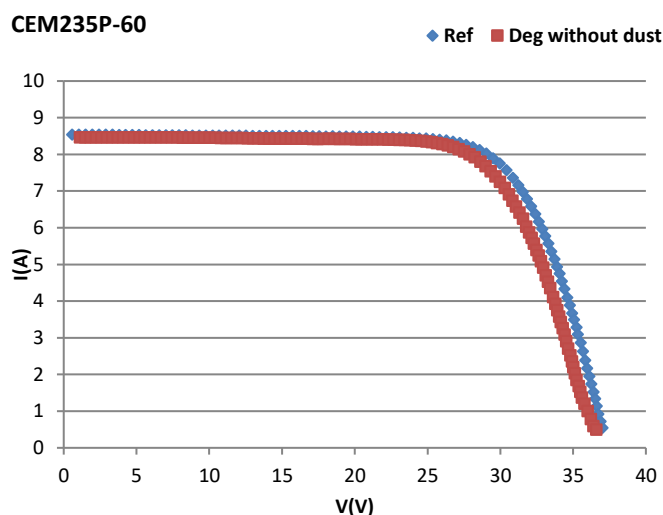


Figure 4. I-V curves for the reference panel and the degraded without dust panel.

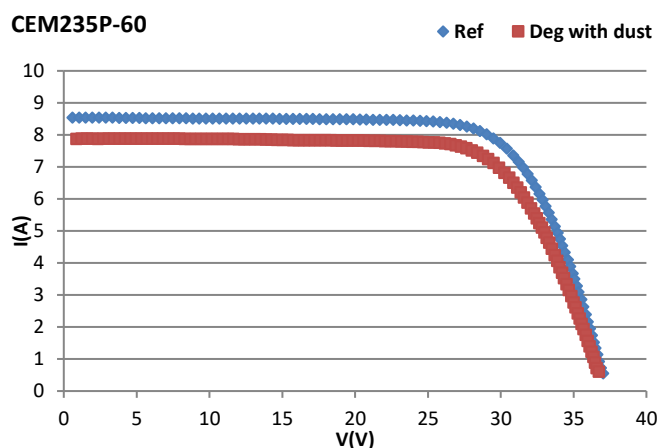


Figure 6. P-V curves for the reference panel and degraded with dust panel.

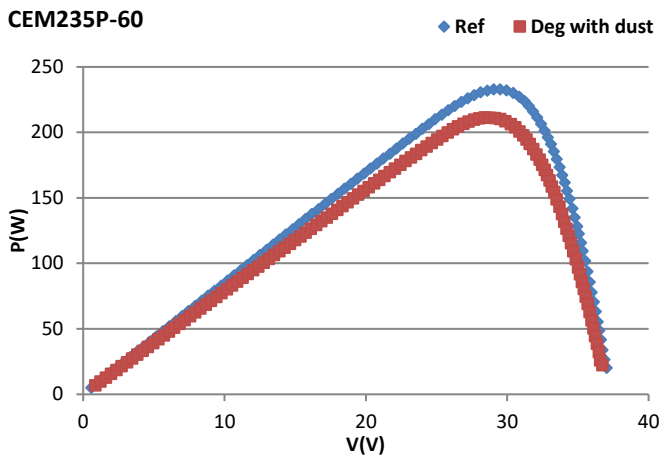


Figure 7. P-V curves for the reference panel and degraded without dust panel.

### 3.2. Degradation mechanisms

Visual analysis was carried out to determine the PV panel degradation modes that took place during the exposed period in the BBA climate. The following defects have been identified:

#### A. Discoloration of capsulant

Discoloration of encapsulant is one of the most prevalent types of visual degradation that has been noted (Figure 8a). Encapsulant discoloration (EVA degradation) occurs when a clear encapsulant turns yellow or even brown, causing the light to transmit towards the solar cells. This phenomenon may lead to the reduction of  $I_{sc}$  module and attenuated power output. According to [Yang & Whitfield, \(2012\)](#), the yellowness index of the encapsulant is proportionally correlated with the degradation of the  $I_{sc}$  of the modules. The performance of the module can be reduced by as much as 50% due to encapsulant browning ([Munoz et al., 2011](#)).

#### B. Snail track

This mode of degradation is one of PV defects (Figure 8b) that can be detected either visually or by EL imaging. It appear as discoloration of the grid fingers of the silicon solar panel front side, resembling a snail track ([Yang & Jiang, 2019](#)). A snail track is caused by discoloration of the silver paste of the front side metallization of silicon solar cells, which occurs at the edge of the solar cell and usually traces invisible cell cracks. Some studies claim that the snail track shortage will show symptoms within 3–5 months ([Meyer et al., 2013](#)), while others claim it could take up to 2 years ([Dobaria et al., 2018](#); [Bouaichi et al., 2019](#)). The cracks are caused by thermal stress and high temperatures, and the presence of moisture seeping through the microcracks causes

the snail track to emerge.

Due to the discoloration of the snail trails, the ability of PV cells to absorb solar irradiance is diminished, which adversely affects the performance of the PV modules. Numerous studies, however, demonstrate that this kind of failure does not significantly lower electrical performance ([Yang et al. 2018](#)). Moreover, the performance of the PV module is mostly impacted by the broken PV cells ([Dolara et al., 2016](#)).

#### C. Hot spot

The hot spot behavior in crystalline silicon solar cells, which has been well reported in many research studies, may result from shading, soiling, damaged cells, or connections (metallization, interconnects), as well as places where high currents flow via resistive zones ([Simon & Mayer, 2010](#)). This type of degradation was noted in the studied panel, as noted in Figure 8c. Hot spots are cell regions with increased temperatures that have the ability to severely degrade modules and hasten the emergence and spread of further failure mechanisms ([Kato, 2011](#)).

#### D. Corrosion

To safeguard the glass borders and provide mounting points for other modules, the majority of commercial modules are enclosed. The most popular frame material is anodized aluminum due to its great strength, low weight, and inexpensive price. Over time, frames may become corroded, deformed, or loose ([Mathiak et al., 2012](#)). Mechanical loading or subpar manufacturing quality can both cause or hasten them. An example of this kind of corrosion was noted in the studied panel, as seen in Figure 8d. The frame degradation mode was a less frequent failure mode than the other failure modes ([Halwachs et al., 2019](#)).

The junction box is a rather typical source of failure in the reported module field failures ([Leva & Aghaei, 2018](#)). Detachment (from the module backsheet), improperly sealed or closed boxes, corrosion, and arcing because of defective or deteriorated wiring are the main failure modes for junction boxes. Figure 8e illustrates the corrosion of the junction box noted in the analyzed panel. Due to the high current levels passing through, junction box component deterioration and failure can result in significant performance losses and safety risks ([Kontges et al., 2014](#)).

The oxidation of metallic contacts such as cell interconnect ribbon was also noted in this panel, as illustrated in Figure 8f. This can be caused by several factors, such as humidity ingress, higher moisture absorption of encapsulant, the combination of higher temperature and humidity, and high system voltage. This defect increases the series resistance and degrades the fill factor, leading to reduced output power ([Kim et al., 2014](#)).

Table 2. The electrical parameters associated with the degradation rate of the used PV panel in STC.

Parameters	Ref Panel	Deg cleaned Panel	Deg with dust Panel	$R_{DC}(\%)$	$R_{DD}(\%)$	$R_{ADC}(\%/y)$	$R_{ADD}(\%/y)$
$I_{sc}$	8.56	8.46	7.87	1.17	8.06	0.23	1.61
$V_{oc}$	37.36	37.02	37.15	0.91	0.56	0.18	0.11
$I_{max}$	7.97	7.88	7.36	1.13	7.65	0.23	1.53
$V_{max}$	28.37	28.37	28.71	3.24	2.08	0.65	0.42
$P_{max}$	233.58	223.49	221.38	4.32	9.5	0.86	1.90

## E. Finger interrupts

The finger interrupts that happen in cell metallization and module connections are also a typical external problem in PV modules. This defect frequently leads to a rise in  $R_s$ , which diminishes power rating (Zafirovska et al., 2017). It was noted in the tested module, as illustrated in Figure 8g. The efficiency of the solar cell is directly impacted by the its finger shape, aging, and fabrication quality (Li et al., 2022).

### 3.3. The five electrical parameters' degradation rate

The values of the characteristic parameters ( $a$ ,  $R_s$ ,  $R_p$ ,  $I_{ph}$ , and  $I_0$ ) of the employed PV panels (degraded (with and without dust) and the reference panel under standard conditions) were evaluated using the extraction method provided by Hussein (2017). There are two steps in this method. The first step is concentrated on the determination of the four parameters namely  $R_s$ ,  $R_p$ ,  $I_{ph}$ , and  $I_0$  using the characterization equations of the points: short-circuit current ( $I_{sc}$ ), open-circuit voltage ( $V_{oc}$ ), and the maximum power  $P_m$  with the corresponding voltage ( $V_m$ ) and current ( $I_m$ ). In the following step, the ideality factor ( $a$ ) value is adjusted by comparing the experimental and simulated I-V curves. The optimization of the NRMSE error was used to accomplish this improvement. This procedure is to be resumed as in the following:

Values of the constants  $A$ ,  $B$ , and  $C$  are assumed to be as follows:

$$A = \exp\left(\frac{V_{oc}}{aV_t}\right) - 1 \quad (3)$$

$$B = \exp\left(\frac{R_s I_{sc}}{aV_t}\right) - 1 \quad (4)$$

$$C = \exp\left(\frac{V_m + R_s I_{max}}{aV_t}\right) - 1 \quad (5)$$

The thermal voltage  $V_t$  is given as:

$$V_t = \frac{a \times N_s \times k \times T}{q} \quad (6)$$

Where  $a$  and  $N_s$  are the diode ideality factor and the number of series-connected solar cells in the panel, respectively.  $q$  and  $k$  are the electron charge and Boltzmann constant, respectively, and  $T$  is the working temperature in Kelvin.

The equations of the specific points cited above can be given as follows (Hussein, 2017):

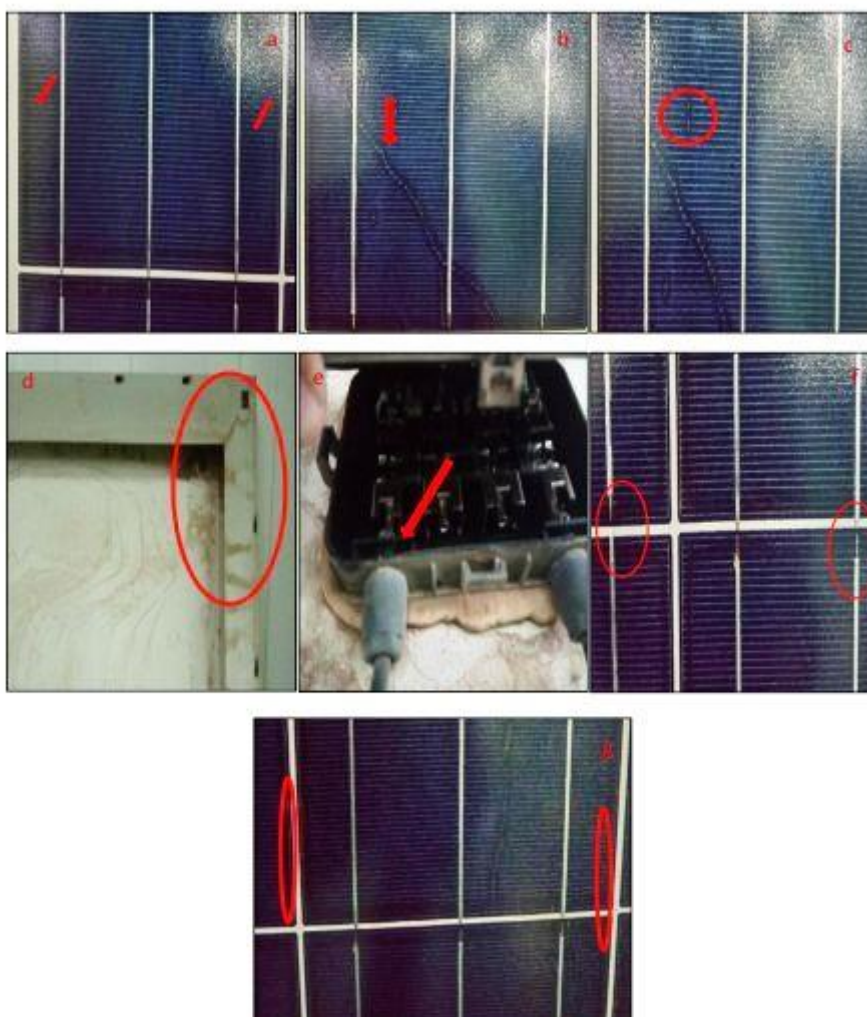


**Figure 8.** Degradation mechanisms recorded.

(a) Discoloration, (b) Snail track, (c) Hot spot, (d) Corrosion of aluminum frame, (e) Corrosion of the junction box, (f) Corrosion of interconnections, and (g) Finger interrupts.

$$I_0 = \frac{I_{ph}}{A} - \frac{V_{oc}}{AR_p} \quad (7)$$

$$I_{sc}(1 + \frac{R_s}{R_p}) = I_{ph} - BI_0 \quad (8)$$

$$I_{max}(1 + \frac{R_s}{R_p}) = I_{ph} - I_0C - \frac{V_{max}}{R_p} \quad (9)$$

By substituting Eq.7 into Eq.9, the following equation is obtained:

$$I_{max}(\frac{R_s+R_p}{R_p}) = I_{ph}(\frac{A-C}{A}) + \frac{CV_{oc}-AV_{max}}{AR_p} \quad (10)$$

By substituting Eq.7 into Eq.8, the following equation is obtained:

$$I_{ph} = \frac{AI_{sc}(1+\frac{R_s}{R_p})-B\frac{V_{oc}}{R_p}}{(A-B)} \quad (11)$$

From Eq.10 and Eq.11, maximum power can be written as follows (Hussein, 2017):

$$I_0(C + \frac{(C+1)V_{max}}{V_t}) - I_{ph} - \frac{2V_{max}}{R_p} = 0 \quad (12)$$

The four parameters namely  $R_s$ ,  $R_p$ ,  $I_0$ , and  $I_{ph}$  are determined by solving the following system of equations, Eq.7, Eq.8, Eq.9, and Eq.12, respectively. These equations can be rearranged to obtain an equation with only one variable,  $R_s$ , as follows (Hussein, 2017):

$$f(R_s) = V_{max}(C + 1)[I_{sc}V_{oc} - I_{sc}V_{max} - I_{max}V_{oc}] - (A - C)I_{sc}V_{max}V_t + (B - C)I_{max}V_{oc}V_t + 2(A - B)I_{max}V_{max}V_t \quad (13)$$

As shown, this equation has one variable only  $R_s$ , and it is easy to find its value using the solver in the Excel software. Once the value of  $R_s$  is determined, the values of  $R_p$  and  $I_{ph}$  are estimated using the following equations (Hussein, 2017):

$$R_p = \frac{(C-B)V_{oc} - (A-B)V_{max}}{(A-B)I_{max} - (A-C)I_{sc}} - R_s \quad (14)$$

$$I_{ph} = \frac{A(1+\frac{R_s}{R_p})I_{sc} - \frac{V_{oc}}{R_p}}{(A-B)} \quad (15)$$

As mentioned in Eq. 7, the value of  $I_0$  is calculated using the estimated values of  $R_p$  and  $I_{ph}$ .

Noting that the four unknown parameters,  $R_s$ ,  $R_p$ ,  $I_{ph}$ , and  $I_0$ , must be calculated using a proposed algorithm, which must be based on an initial value of the ideality factor  $a_0$ . The optimum values of these four parameters are then determined by minimizing the Normal Root Mean Square Error (NRMSE) between measured current ( $I_m$ ) and simulated current ( $I_s$ ) values, as noted as an objective function. The NRMSE is calculated as follows (Maouhoub, 2018):

$$NRMSE(\%) = \frac{100}{\sum_{i=1}^N I_{m,i}} \times \left( \frac{\sum_{i=1}^N (I_{m,i} - I_{s,i})^2}{N} \right)^{0.5} \quad (16)$$

The values  $I_{m,i}$  and  $I_{s,i}$  are the measured and simulated currents of the  $i^{th}$  point, respectively, and  $N$  is the total number of experimental points used.

A program in the Excel software was developed to perform the determination of all these parameters for the three panels studied. The values of the five parameters are gathered in Tableau 3 for the reference panel and the degraded panel (both with and without dust) in the standard conditions.

Figures 9, 10, and 11 show the validity of these findings by comparing the experimentally measured and simulated curves (I-V and P-V) for the three panels (reference, degraded ones (with and without dust)). It should be noted that the Hussein method accurately defines the parameters ( $a$ ,  $R_s$ ,  $R_p$ ,  $I_{ph}$ , and  $I_0$ ).

The reference panel has a coefficient of determination ( $R^2$ ) of 0.9999, an NRMSE value of 0.00813% for I-V curve, a  $R^2$  value of 0.9995, and an NRMSE value of 0.0147% for P-V curve. The degraded panel without dust revealed 0.9995 ( $R^2$ ) and 0.026% (NRMSE) values for the I-V curve and 0.9897 ( $R^2$ ) and 0.0588% (NRMSE) values for the P-V curve. The degraded panel with dust showed 0.9999( $R^2$ ) and 0.004% (NRMSE) values for the I-V curve, and 1 ( $R^2$ ) and 0.006% (NRMSE) values for the P-V curve.

For each of the five parameters ( $a$ ,  $R_s$ ,  $R_p$ ,  $I_{ph}$ , and  $I_0$ ), the degradation rate and annual degradation rate are determined in order to investigate the effects of degradation and dust on those parameters. As noted in Table 3, degradation and the presence of dust have an effect on the five parameters.

The ideality factors( $a$ ) including degradation rate and annual degradation rate were 7.93% and 1.59%/y, respectively. When dust is present, this factor increases by 4.18%, reaching 11.77% (2.36%/y). The  $I_{ph}$  degraded rate is the lowest at 1.04% (0.21%/y); then, it increases to 7.96% (1.98%/y) with a pourcentage of 6.99% in the presence of dust. However, when the  $I_0$  degradation rate is the highest at 76.87% (18.53%/y), it jumps to 92.64% (18.53%/y), with a rise of 68.17% due to the presence of dust.

**Table 3.** The electrical parameters associated with the degradation rate of the used PV panel in STC.

Parameters	Ref Panel	Deg cleaned Panel	Deg with dust Panel	$R_{DC}(\%)$	$R_{DD}(\%)$	$R_{ADC}(\%/y)$	$R_{ADD}(\%/y)$
a	1.274	1.173	1.124	7.93	11.77	1.59	2.35
$R_s$	0.3254	0.4502	0.4705	-38.35	-44.59	-7.67	-8.92
$R_p$	372.5177	341.2018	409.4662	8.41	-9.92	1.68	1.98
$I_{ph}$	8.56	8.4712	7.879	1.04	7.96	0.21	1.59
$I_0$	4.63011x10 <sup>-8</sup>	10171x10 <sup>-8</sup>	3.80x10 <sup>-9</sup>	76.87	92.64	15.37	18.53

The  $R_s$  increased during this time; its degradation rate was -38.35%, with an annual rate of -7.67%/y, and this can be related to the detected degradation mechanisms (oxidation of metallic contacts and finger interrupts, as described in Section 3.3) and inducing power degradation, as noted in Table 2. In arid climates, the same evolution of  $R_s$  resistance was observed (Younes et al., 2020), but with much high values ranging from 137.84% to 229.73%. When dust is present, this  $R_s$  degradation decreases to -44.59% (-8.92%/y), with the decrease of 4.51%. In this case, the dust acts as a barrier between the PV and the radiation, reducing the transmittance of cellular glazing (Chaichan et al., 2015) and the output power, as shown in Table 2.

The  $R_p$  degradation rate was 8.41%, with an annual rate of 1.68%/y. A similar decrease in  $R_p$  was seen in a desert climate (Younes et al., 2020), with an elevated value of 65%. The decrease in  $R_p$  contributes to the current reduction (Younes et al., 2020), hence the decrease in the power, maximum voltage, and maximum current, as noted in Table 2. Due to the impact of dust being present, the mentioned rate degraded by -9.92% (-1.98%/y), with a -20.01% decrease, which increased the current, as shown in Figure 6 compared with Figure 4.

The climate conditions of the BBA region across the six-year study period have a variable impact on the five characteristic parameters of the panels.  $I_0$  is the parameter most affected by the mentioned conditions, followed by resistance  $R_s$ , which degrades at a negative rate, followed by  $R_p$  and  $a$ , which degrade at a similar rate, and finally  $I_{pv}$ , which degrades at the slowest rate. These degradation rates vary when dust is present on the PV panel.  $I_0$  suffers another degradation (severe) on the order of 68.17%. The resistance  $R_p$  rises by 20.01%, the  $I_{pv}$  deteriorates by 6.99%, and the resistance  $R_s$  rises by 4.51%, as well. The ideality factor ( $a$ ) has decreased by 4.18%.

## 5. CONCLUSIONS

Photovoltaic module performance was found to be susceptible to the climate, particularly in desert areas. In addition to these climate factors, dust collection is another problem that has an

impact on the functioning of the PV system. Noting that the desert areas are not the only ones with this problem, this study considers the impact of dust on the degraded panels under outdoor conditions in an industrial zone in the BBA (Algeria) region with a continental climate. The degradation rate and the annual degradation rate of the five parameters characterizing the behavior of a degraded PV panels were carried out for the first time.

In order to analyze the I-V and P-V curves for the tested panels and to identify the degraded mechanisms noticed under this climate after six years of exposure, three panels including SEM235P-60 (degraded panels (with and without dust) and a reference panel) were examined.

The power degradation rate for the degraded panel without dust was 4.32% (0.86%/y), which was comparable to the literature finding and lower than the results observed in desert regions.  $V_{max}$  had the highest rate of degradation rate (3.24%-0.65%/y), followed by  $I_{sc}$  (1.17%-0.23%/y) and  $I_{max}$  (1.17%-0.23%/y) with comparable degradation rates, while  $V_{oc}$  had the lowest rate of degradation (0.91% (0.18%/y)). These degradation rates were related to the mechanisms of degradation identified in the tested panel.

For the degraded panel with dust, the power degradation rate was 9.50% (1.90%/y), with an increase of 5.45% compared to the panel without dust. The  $V_{oc}$  degradation rate was 0.56% (0.11%/y) with a non-significant degradation of 0.35% in the presence of dust.  $I_{sc}$  (8.06%-1.61%/y) and  $I_{max}$  (7.65%-1.53%/y) experienced the highest degradation rates, with 6.97% and 6.0% increases in the presence of dust, respectively. The  $V_{max}$  degradation rate was 2.08% (0.42%/y), with a reduction of 1.20% compared to the panel without dust.

The determination of the five parameters ( $a$ ,  $R_s$ ,  $R_p$ ,  $I_0$ , and  $I_{pv}$ ) of the PV panels studied was carried out according to the Hussien model. This model is quite effective for both the reference panel and the gradient panels (with and without dust). With the help of these results, the degraded rate and annual degraded rate of the five characteristics, as well as how dust affects these parameters, were determined.

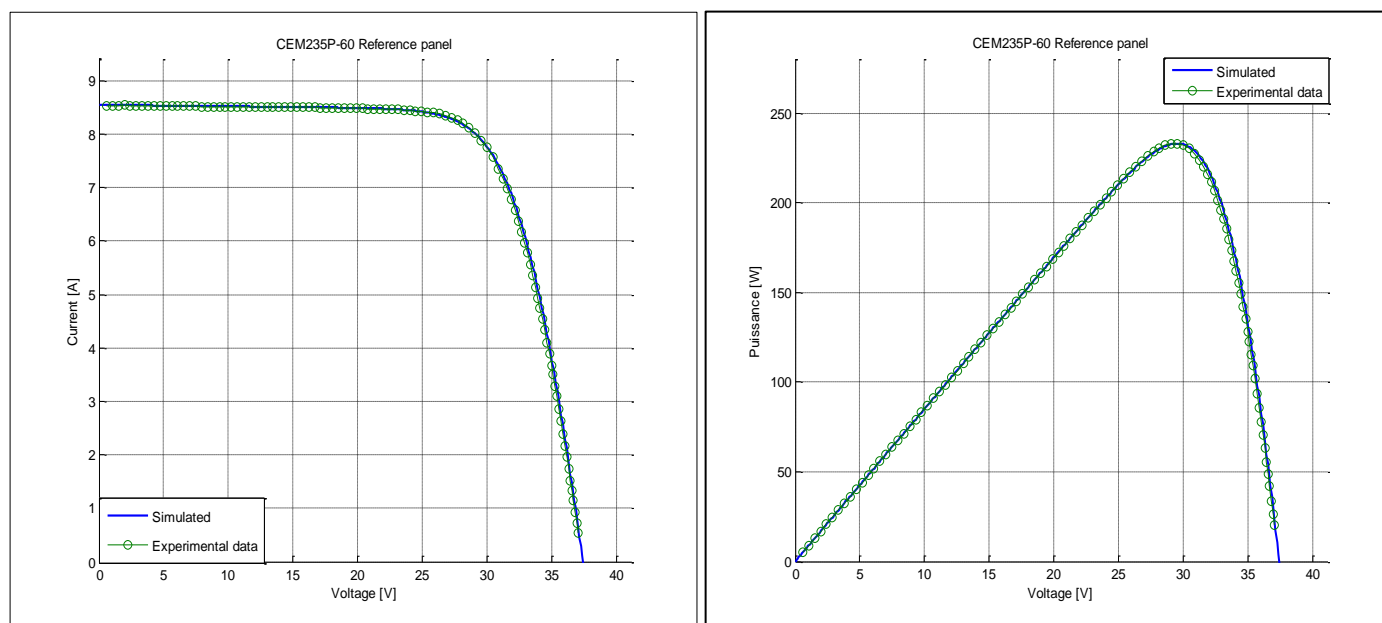
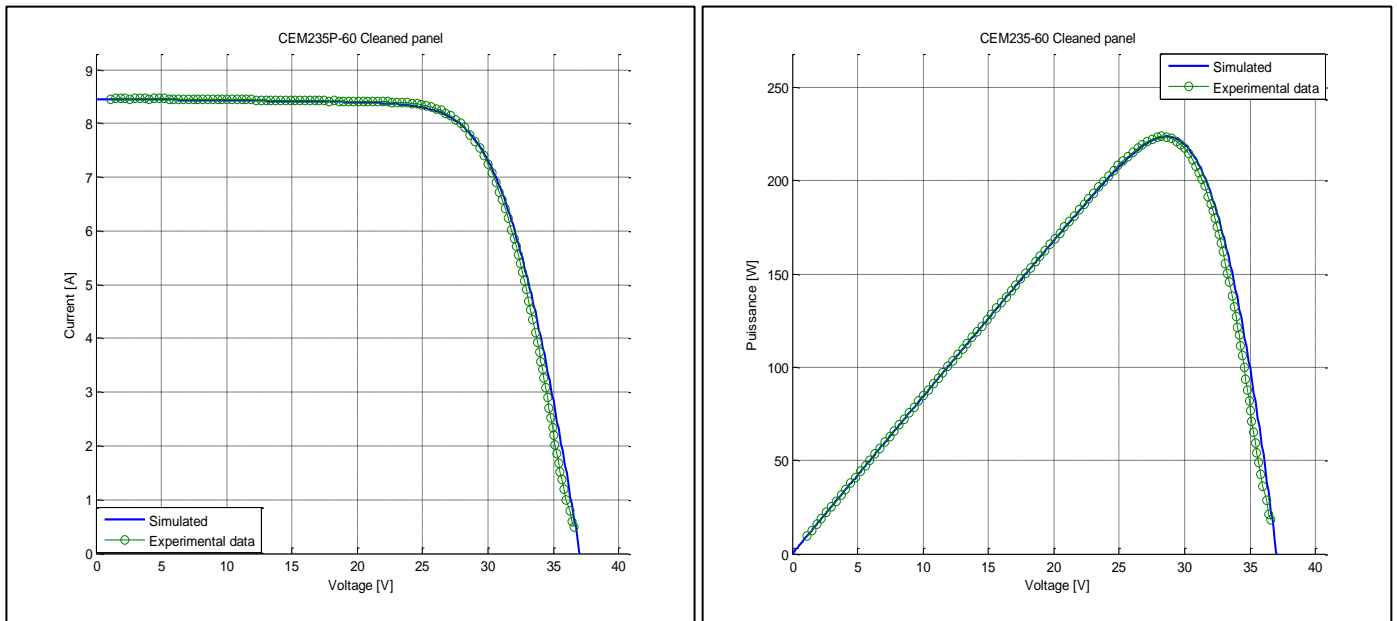
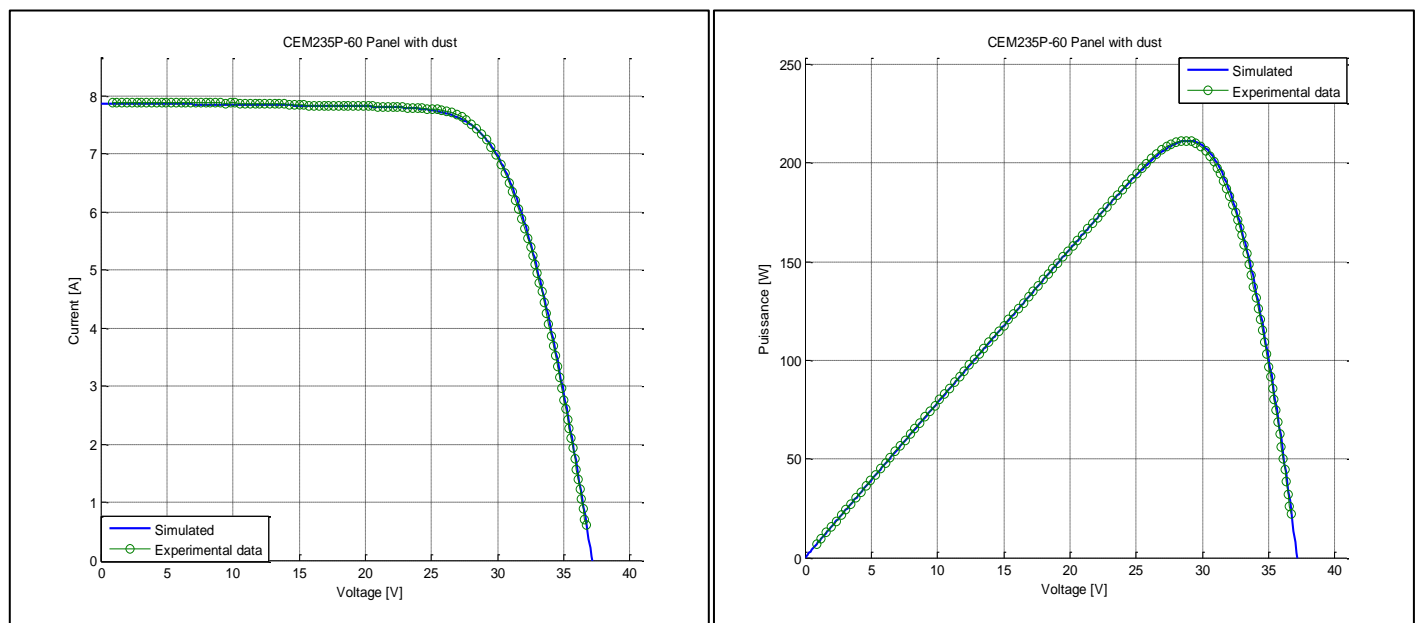


Figure 9. Comparison of the measured and simulated curves (I-V and P-V) for the reference panel.



**Figure 10.** Comparison of the measured and simulated curves (I-V and P-V) for the degraded panel without dust.



**Figure 11.** Comparison of the measured and simulated curves (I-V and P-V) for the degraded panel with dust.

The degraded panel without dust had an ideality factor(a) degraded rate of 7.93% and (1.59%/y). This factor rose by 4.18% when dust was present, reaching 11.77% (2.36%/y). The  $I_{ph}$  degradation rate was the lowest at 1.04% (0.21%/y); then, it increased to 7.96% (1.98%/y), which is 6.99%, in the presence of dust. However, the  $I_0$  degradation rate was the highest at 76.87% (18.53%/y) and jumped to 92.64% (18.53%/y) with a rise of 68.17% when dust was present.

The degradation rate of the  $R_s$  was -38.35% (-7.67%/y), which could be attributed to the indicated degradation mechanisms, and it caused power degradation. When dust was present, the  $R_s$  degradation decreased to -44.59% (-8.92%/y), which is a 4.51% decrease. In this instance, the dust acts as a shield between the PV and the radiation, reducing the cellular glazing transmittance and as a result, the output power is reduced  $R_p$

degradation rate was reduced by 8.41% (1.68%/year), which was related to the loss of current and consequently power (maximum voltage and maximum current). In the presence of dust,  $R_p$  degradation rate was -9.92% (-1.98%/year), with a drop of -20.01% compared to the absence of dust.

The appropriateness of netoiling methods must be considered because dust, even in non-desert climates, has a significant impact on the electrical characteristics of a PV panel.

## 6. ACKNOWLEDGEMENT

The authors would like to thank all the staff of the BBA Condor Society for providing access and their help during the realization of this work.

## NOMENCLATURE

$N_s$	Number of cells
$P$	Generated power by the PV module [W]
$P_{max}$	Maximum power [W]
$q$	Electronic charge ( $1.6 \times 10^{-16}$ C)
$R^2$	Coefficient of determination
$R_{ADC}$	Annual degradation rate of the degraded panel without dust [%/Y]
$R_{ADD}$	Annual degradation rate of the degraded panel with dust [%/Y]
$R_{DC}$	Degradation rate of the degraded panel without dust [%]
$R_{DD}$	Degradation rate of the degraded panel with dust [%]
$R_p$	Shunt resistance [ $\Omega$ ]
$R_s$	Series resistance [ $\Omega$ ]
$T$	Cell temperature [K]
$V$	Generated voltage [V]
$V_{max}$	Maximum power tension [V]
$V_{oc}$	Open circuit voltage [V]
$V_t$	Thermal voltage

## REFERENCES

- Ahmadi, N., Rezazadeh, S., Dadvand, A., & Mirzaee, I. (2015). Numerical Investigation of the Effect of Gas Diffusion Layer with Semicircular prominences on Polymer Exchange Membrane Fuel Cell Performance and Species Distribution. *Journal of Renewable Energy and Environment*, 2(2), 36-46. <https://doi.org/10.30501/jree.2015.70069>.
- Aïssa, B., Isaïfan, R. J., Madhavan, V. E., & Abdallah, A. A. (2016). Structural and physical properties of the dust particles in Qatar and their influence on the PV panel performance. *Scientific Reports*, 6(1), 1–12. <https://doi.org/10.1038/srep31467>.
- Amer, A., Abdelsalam A., Yashar A., Mamdouh E. H. A., Shubham, Sh., Reza A. (2022). Reducing PV soiling and condensation using hydrophobic coating with brush and controllable curtains. *International Journal of Low-Carbon Technologies*, 17, 919–930. <https://doi.org/10.1093/ijlct/ctac056>
- Andrea, Y., Pogrebnya, T., and Kichonge. B. (2019). Effect of Industrial Dust Deposition on Photovoltaic Module Performance: Experimental Measurements in the Tropical Region. *Hindawi International Journal of Photoenergy*. <https://doi.org/10.1155/2019/1892148>
- Ashkan, T., S. Mehdi, P., Farzin, R., Nima, A., Hadi, Shahmohammadi. (2014). Design of Innovative Channel Geometrical Configuration and Its Effect on Species Distribution. *Journal of Renewable Energy and Environment*, 1(1), 20-29. <https://doi.org/10.30501/jree.2014.70053>.
- Bandou, F., Hadj Arab, A., Belkaid. M.S., Logerais. P.O., Riou. O., et al. (2015). Evaluation performance of photovoltaic modules after a long time operation in Saharan environment. *International Journal of Hydrogen Energy*, 40, 13839–13848. <http://dx.doi.org/10.1016/j.ijhydene.2015.04.091>
- Belhaouas, N., Mehareb, F., Kouadri-Boudjelthia, E., Assem, H., Bensalem, S., Hadjrioua, F., Aissaoui, A., Hafdaoui, H., Chahtou, A., Bakria, K., Saheb-Koussa, D. (2022). The performance of solar PV modules with two glass types after 11 years of outdoor exposure under the Mediterranean climatic conditions. *Sustainable Energy Technologies and Assessments*, 49(101771), <https://doi.org/10.1016/j.seta.2021.101771>
- Bouaichi, A., Alami M. A. Hajjaj, Ch., Messaoudi, C., Ghennioui, A., Benlarabi, A., Ikken, B., El Amrani, A., Zitouni, H. (2019). In-situ evaluation of the early PV module degradation of various technologies under harsh climatic conditions: The case of Morocco. *Renewable Energy*, 143(C), 1500-1518. <https://doi.org/10.1016/j.renene.2019.05.091>.
- Chaichan, M.T., Abass, K.I., Kazem, H.A. (2018). Energy yield loss caused by dust and pollutants deposition on concentrated solar power plants in Iraq weathers. *International Research Journal Advanced Engineering Science*, 3, 160-169. <https://web.archive.org/web/20180410180634/http://irjaes.com/pdf/V3N1Y17-IRJAES/IRJAES-V3N1P621Y18.pdf>
- Chaichan, M.T., Kazem, H.A. (2016). Experimental analysis of solar intensity on photovoltaic in hot and humid weather conditions. *International Journal Scientific and Engineering Research*, 7, 91-96. <https://web.archive.org/web/20180410180634/http://irjaes.com/pdf/V3N1Y17-IRJAES/IRJAES-V3N1P621Y18.pdf>
- Chaichan, M.T., Mohammed, B.A., Kazem, H.A. (2015). Effect of Pollution and Cleaning on Photovoltaic Performance Based on Experimental Study. *International Journal Scientific and Engineering Research*, 6(4), 594-601. <https://www.uotechnology.edu.iq/paper/PDF/power/No.%2020.pdf>
- Chen, J., Pan, G., Ouyang, J., Ma, J., Fu, L., Zhang, L. (2020). Study on impacts of dust accumulation and rainfall on PV power reduction in East China. *Energy*, 194. <https://doi.org/10.1016/j.energy.2020.116915>.
- Condor. (2022). Catalogue Produits Solar Photovoltaïques. Available from: [https://www.condor.dz/images/pdf/CatalogueProduitsSolairePhotovoltaïques\\_min.pdf](https://www.condor.dz/images/pdf/CatalogueProduitsSolairePhotovoltaïques_min.pdf)
- Darwish, Z.A., Kazem, H.A., Sopian, K., Alghoul, M.A., Chaichan, M.T. (2013). Impact of some environmental variables with dust on solar photovoltaic (PV) performance: review and research status. *Researchgate*. Net 7, 152-159. <https://doi.org/10.1021/ie301985y>.
- Dobaria, B.V., Sharma, V., Deshara, A. A. (2018). Investigation of failure and degradation types of solar PV plants in a composite climate: abstract after 4-6 Years of field operation, in: *Advances in Smart Grid and Renewable Energy*, Springer, Singapore, 227-235. [https://doi.org/10.1007/978-981-10-4286-7\\_22](https://doi.org/10.1007/978-981-10-4286-7_22).
- Dolara, A., Lazaroiu, G.C., Leva, S., Manzolini, G., Votta, L. (2016). Snail trails and cell microcrack impact on PV module maximum power and energy production. *IEEE Journal of Photovoltaic*, 6(5), 1269–77. <https://doi.org/10.1109/JPHOTOV.2016.2576682>
- Dorobantu, L., Popescu, M.O., Popescu, C.I., Craciunescu, A. (2017). The effect of surface impurities on photovoltaic panels. *Renewable Energy Power Quality Journal*, 1, 622-626. <https://doi.org/10.24084/repqj09.405>.
- El-Shobokshy, S., Hussein, F.M. (1993). Effect of dust with different physical properties on the performance of photovoltaic cell. *Solar Energy*, 51(6), 505-511. [https://doi.org/10.1016/0038-092X\(93\)90135-B](https://doi.org/10.1016/0038-092X(93)90135-B)
- Essalaimeh, S., Al-Salaymeh, A., Abdullat, Y. (2013). Electrical production for domestic and industrial applications using hybrid PV-wind system. *Energy Conversion Management*, 65, 736-743. <https://doi.org/10.1016/j.enconman.2012.01.044>
- Franzese, N., Dincer, I., Sorrentino, M., A. (2020). New multigenerational solar-energy based system for electricity, heat and hydrogen production. *Applied Thermal Engineering*, 171, No 115085. <https://doi.org/10.1016/j.applthermaleng.2020.115085>.
- Hachicha, A.A., Al-Sawafta, I., Said, Z. (2019). Impact of dust on the performance of solar photovoltaic (PV) systems under United Arab Emirates weather conditions. *Renewable Energy*, 141, , 287-297. <https://doi.org/10.1016/j.renene.2019.04.004>.
- Halwachs, M., Neumaier, L., Vollert, N., Maul, L., Dimitriadis, S., Voronko, Y., et al. (2019). Statistical evaluation of PV system performance and failure data among different climate zones. *Renewable Energy*, 139, 1040–60. <https://doi.org/10.1016/j.renene.2019.02.135>.
- Hussein, A. M. (2017). Extraction of Unknown Parameters of PV Modules", 9th IEEE-GCC Conference and Exhibition (GCCCE). <https://doi.org/10.1109/ieeegcc.2017.8448245>
- Ihaddadene, R., Jed, M.E.H., Ihaddadene, N., Souza. A. (2022). Analytical assessment of Ain Skhoua PV plant performance connected to the grid under a semi-arid climate in Algeria. *Solar Energy*, 232, 52–62. <https://doi.org/10.1016/j.solener.2021.12.055>.
- Kahoul, N., Chenni, R., Cheghib, H., Mekhilef, S. (2017). Evaluating the reliability of crystalline silicon photovoltaic modules in harsh environment. *Renewable Energy*, 109, 66–72. <https://doi.org/10.1016/j.renene.2017.02.078>.
- Kato, K. (2011). PVResQ!: a research activity on reliability of PV systems from an user's viewpoint in Japan. In: Dhre NG, Wohlgemuth JH, Lynn KW, editors. 81120K. <https://doi.org/10.1117/12.896135>.

27. Kazem, H.A., Chaichan, M.T., Alwaeli, A.H., Mani, K. (2017). Effect of shadows on the performance of solar photovoltaic, Mediterranean green buildings and renewable energy", *selected papers from the world renewable energy network's med green forum*. [https://doi.org/10.1007/978-3-319-30746-6\\_27](https://doi.org/10.1007/978-3-319-30746-6_27).
28. Kim, J.H., Park, J., Kim, D., Park, N. (2014). Study on mitigation method of solder corrosion for crystalline silicon photovoltaic modules. *International Journal of Photoenergy*, <http://dx.doi.org/10.1155/2014/809075>.
29. Kimber, A., Mitchell, L., Nogradi, S., Wenger, H. (2007). The effect of soiling on large grid-connected photovoltaic systems in California and the Southwest Region of the United States. *Conf. Rec. 2006 IEEE 4th World Conf. Photovolt. Energy Conversion, WCPEC- 4 2*, 2391-2395 <https://doi.org/10.1109/WCPEC.2006.279690>.
30. Kontges, M., Kurtz, S., Packard, CE., Jahn, U., Berger, K., Kato, K., et al. (2014). Review of failures of photovoltaic modules. *IEA PVPS Task 13 External final report IEA-PVPS*. <https://doi.org/978-3-906042-16-9>.
31. Li, L., Tu, J., Wu, J., Hu, K., Yu, S. (2022). Effect of finger interruption mode on the performance of crystalline silicon solar cells. *Solar Energy*, 238(15), 381-391. <https://doi.org/10.1016/j.solener.2022.03.065>.
32. Leval, S., Aghaei M. (2018). Failures and defects in PV systems review and methods of analysis. In: Badescu Viorel, George Cristian Lazaroiu LB, editors. *Power Eng. Adv. Challenges Part B Electr. Power*. first ed. CRC Press; 56–84. <https://re.public.polimi.it/handle/11311/1073064>
33. Maouhoub, N. (2018). Photovoltaic module parameter estimation using an analytical approach and least squares method. *Journal of Computational Electronics*, Vol. 17, No 2, 784–790. <https://doi.org/10.1007/s10825-017-1121-5>.
34. Mani, M., Pillai, R. (2010). Impact of Dust on Solar Photovoltaic (PV) Performance: Research Status, Challenges and Recommendations. *Renewable and Sustainable Energy Reviews*, 14(9), 3124-3131. <https://doi.org/10.1016/j.rser.2010.07.065>
35. Mathiak, G., Althaus, J., Menzler, S., Lichtschlager, L., Herrmann, W. (2012). PV Module Corrosion from ammonia and salt mist - experimental study with full-size modules. In: 27th Eur. Photovolt. *Sol. Energy conf. Exhib. WIP*, 3536–40. <https://doi.org/10.4229/27thEUPVSEC2012-4BV.3.44>.
36. Menoufi, K. (2017). Dust accumulation on the surface of photovoltaic panels: introducing the photovoltaic soiling index (PVSI). *Sustainability*, 9(6). <https://doi.org/10.3390/su9060963>.
37. Meyer, S., Richter, S., Timmel, S., Glaser, M., Werner, M., Swatek, S., Hagendorf, C. (2013). Snail trails: root cause analysis and test procedures ", *Energy Procedia*. 38, 498-505. <https://doi.org/10.1016/j.egypro.2013.07.309>.
38. Munoz, M.A., Alonso-Garcia, M.C., Vela, N., Chenlo, F. (2011). Early degradation of silicon PV modules and guaranty conditions. *Solar Energy*, 85, 2264–2274. <https://doi.org/10.1016/j.solener.2011.06.011>.
39. Namdari, S., Karimi, N., Sorooshian, A., Mohammadi, G.H., Sehatkashani, S. (2018). Impacts of climate and synoptic fluctuations on dust storm activity over the Middle East. *Atmospheric Environment*, 173, 265-276. <https://doi.org/10.1016/j.atmosenv.2017.11.016>.
40. Pan, A., Lu, H., and Zhang, L.-Z. (2019). Experimental investigation of dust deposition reduction on solar cell covering glass by different self-cleaning coatings. *Energy*, 181, 645–653. <https://doi.org/10.1016/j.seta.2018.12.024>.
41. Sahu, S.K., Singh K. A., Natarajan, S.K. (2021). Electricity generation using solar parabolic dish system with thermoelectric generator—An experimental investigation, *Heat Transfer*, 1-14. <https://doi.org/10.1002/hjt.22253>.
42. Sendhil, K. N., Subbarama, K. S., Elavarasan. E and Arjun Singh. K. (2019). Performance analysis of solar photovoltaic panel at Karaikal weather conditions. *IOP Conference Series: Earth and Environmental Science*, 312, , 312012013. <https://doi.org/10.1088/1755-1315/312/1/012013>.
43. Simon, M., Meyer, EL. (2010). Detection and analysis of hot-spot formation in solar cells. *Solar Energy Materials and Solar Cells*, 94, 106–113. <https://doi.org/10.1016/j.solmat.2009.09.016>.
44. Styszko, K., Jaszczur, M., Teneta, J., et al., (2019). An analysis of the dust deposition on solar photovoltaic modules. *Environmental Science Pollution Reserch*, 26(9), 8393–8401. <http://dio.org/10.1007/s11356-018-1847-z>.
45. Subbarama, K. A., Gudapati, K., Gummalla, V. S. R., and Sendhil K. N. (2019). A short review on recent trends and applications of thermoelectric Generators. *IOP Conferences Series: Earth Environmental Sciences*, 312 012013. <https://doi.org/10.1088/1755-1315/312/1/012013>.
46. Tanesab, J., Parlevliet, D., Whale, J., and Urmee, T. (2019). The effect of dust with different morphologies on the performance degradation of photovoltaic modules. *Sustainable Energy Technologies Assessments*, 31, 347–354. <https://doi.org/10.1016/j.seta.2018.12.024>.
47. Tripathi, A. K., Aruna, M., and Murthy, C. S. N. (2017). Performance of a PV panel under different shading strengths. *International Journal of Green Energy*, 40(3), 248–253. <https://doi.org/10.1080/01430750.2017.1388839>.
48. Vidyanandan K. (2017). An Overview of Factors Affecting the Performance of Solar PV Systems. 27, *Energy Scan House J Corp Plan NTPC Ltd, New Delhi*. [https://www.researchgate.net/profile/Kv-Vidyanandan/publication/319165448\\_An\\_Overview\\_of\\_Factors\\_Affecting\\_the\\_Performance\\_of\\_Solar\\_PV\\_Systems/links/5996ae170f7e9b91cb10967b/An-Overview-of-Factors-Affecting-the-Performance-of-Solar-PV-Systems.pdf](https://www.researchgate.net/profile/Kv-Vidyanandan/publication/319165448_An_Overview_of_Factors_Affecting_the_Performance_of_Solar_PV_Systems/links/5996ae170f7e9b91cb10967b/An-Overview-of-Factors-Affecting-the-Performance-of-Solar-PV-Systems.pdf)
49. Waved, W., et al., (2017). Characterization of dust accumulated on photovoltaic panels in Doha, Qatar. *Solar Energy*, 142, 123-135. <https://doi.org/10.1016/j.solener.2016.11.053>.
50. Weather Spark. (2022). Weather conditions in BBA. Available from: <https://fr.weatherspark.com/y/50132/M%C3%A9%20C3%A9%20moyenne-%20Bordj-Bou-Argeridj-Alg%C3%A9rie-tout-au-long-de-l'ann%C3%A9e>.
51. Wikipedia. (2022). Geographica Situation of BBA. Available from: [https://fr.wikipedia.org/wiki/Wilaya\\_de\\_Bordj\\_Bou\\_Argeridj](https://fr.wikipedia.org/wiki/Wilaya_de_Bordj_Bou_Argeridj).
52. Yang, H., He, W., Wang, H., Huang, J., Zhang, J. (2018). Assessing power degradation and reliability of crystalline silicon solar modules with snail trails. *Solar Energy Materials Solar Cells*, 187, 61–8. <https://doi.org/10.1016/j.solmat.2018.07.021>.
53. Yang, S., and Jiang, L. (2019). Crystalline Silicon PV Module Field Failures. Durability and Reliability of Polymers and Other Materials in Photovoltaic Modules, 177-216. <https://doi.org/10.1016/B978-0-12-811545-9.00008-2>.
54. Yang, S., Whitfield, K. (2012). Thermal Endurance Study of Polymers Used in Low Concentration Photovoltaic Modules", *Journal of Photonics for Energy*, 2(1). <https://doi.org/10.1117/1.JPE.2.021803>.
55. Younes, M., Labeled, D., Kahoul, N., Cheghib, H., Kherici, Z., Affari, B. C., & De Cardona, M. S. (2020). Silicon solar cells performance in Algerian desert. *11th International Renewable Energy Congress (IREC)*. <https://doi.org/10.1109/irec48820.2020.9310366>.
56. Zafifirovska, I., Juhl, M.K., Weber, J.W., Wong, J., Trupke, T. (2017). Detection of Finger Interruptions in Silicon Solar Cells Using Line Scan Photoluminescence Imaging. *IEEE Journal of Photovoltaic*, 7, 1496–1502. <https://doi.org/10.1109/JPHOTOV.2017.2732220>.